Atherosclerosis 407 (2025) 120412

Contents lists available at ScienceDirect

Atherosclerosis

journal homepage: www.elsevier.com/locate/atherosclerosis

Differential effects of traditional cigarette, electronic cigarette, and tobacco heating product on human vascular smooth muscle cell phenotypic switch: A comparative functional perspective

L. Bianchi [a], I. Damiani [b,1], R. De Salvo [a], C. Rossi [b], A. Carleo [c], C. D'Alonzo [b], L. Bini [a], A. Corsini [b,d], S. Bellosta [b,d,*]

[a] Laboratory of Functional Proteomics – Department of Life Sciences, Siena University, 53100, Siena, Italy
[b] Department of Pharmacological and Biomolecular Sciences "Rodolfo Paoletti", Università degli Studi di Milano, via Balzaretti 9, 20133, Milan, Italy
[c] Laboratory of Molecular Medicine and Genomics, Department of Medicine, Surgery and Dentistry "Scuola Medica Salernitana", University of Salerno, 84081, Baronissi, Italy
[d] Centro di Ricerca Coordinata sulle Interazioni Farmacologiche, Università degli Studi di Milano, via Balzaretti 9, 20133, Milan, Italy

ARTICLE INFO

Keywords:
Smooth muscle cells
Cigarette smoke
E-Cigarette
Tobacco heating products
Osteogenic-like phenotype
Calcification
MMP3

ABSTRACT

Background and aims: Vascular smooth muscle cell (SMC) phenotypic switching, from a contractile to a synthetic state, impacts on atherosclerotic plaque development. While traditional cigarette (TC) smoke is a known driver of cardiovascular disease, the effects of alternative nicotine delivery systems, i.e. electronic cigarettes (E-cigs) and tobacco heating products (THPs), on SMC behavior remains poorly understood. We evaluated the effects of water-soluble components collected in aqueous extracts (AEs) from TC, E-cig, and THP smoke, on human aortic SMC (HASMC) phenotypic switch.

Methods: HASMCs were treated for 48 h with the three AEs. Gene expression and protein abundance profiles were assessed to evaluate cell phenotypic modulation, proliferation, migration, extracellular matrix remodeling, and inflammatory responses. Label-free MS/MS proteomic analysis and wound healing assays were also used to further characterize cellular responses.

Results: Different AEs induced distinct gene expression and protein patterns, but all seemed to induce a hybrid contractile-synthetic phenotype. TC and THP extracts increased *MMP3* expression, whereas E-cig AE down-regulated *MMPs*. E-cig extracts, although reducing inflammatory cytokines, enhanced HASMC proliferation and migration, *bona fide* by upregulating PCNA, RAC1, and ROCK2, thus suggesting an increased vascular remodeling. Proteomic analysis indicated mitochondrial dysfunction and redox imbalances further advising about distinct, harmful effects of AEs on vascular health and atherosclerotic lesion progression.

Conclusion: Our findings revealed complex differential molecular effects of TC, E-cig, and THP AEs on HASMC biology, emphasizing the necessity for further research to assess their actual long-term cardiovascular implications.

1. Introduction

Vascular smooth muscle cells (SMCs) constitute the major cells in the arterial media layer, playing a key role in atherogenesis contributing to plaque stability by preventing fibrous cap rupture [1]. Unlike terminally differentiated myocardial and skeletal muscle cells, mature SMCs can adapt their phenotype in response to environmental stresses [2], such as vascular injury or altered blood flow [3,4]. During atherosclerosis, SMCs undergo phenotypic modulation, transitioning from a contractile to a synthetic phenotype characterized by increased proliferation,

* Corresponding author. Department of Pharmacological and Biomolecular Sciences "Rodolfo Paoletti", Università degli Studi di Milano, via Balzaretti 9, 20133, Milan, Italy.

E-mail addresses: laura.bianchi@unisi.it (L. Bianchi), isabella.damiani@unimi.it (I. Damiani), rossana.desalvo@unisi.it (R. De Salvo), clara.rossi@unimi.it (C. Rossi), alfonsocarleo@yahoo.it (A. Carleo), camilla.dalonzo@studenti.unimi.it (C. D'Alonzo), luca.bini@unisi.it (L. Bini), alberto.corsini@unimi.it (A. Corsini), stefano.bellosta@unimi.it (S. Bellosta).

[1] Present address: Division of Cardiovascular Medicine, Stanford University School of Medicine, Stanford, CA 94305, USA.

https://doi.org/10.1016/j.atherosclerosis.2025.120412
Received 22 January 2025; Received in revised form 11 June 2025; Accepted 11 June 2025
Available online 24 June 2025

migration, cytokine secretion, and extracellular matrix (ECM) production, as well as macrophage or fibroblast markers [5–8]. SMCs undergoing phenotypic modulation exhibit a shift in gene expression toward a fibroblast-like phenotype, with a marked upregulation of fibronectin (*FN1*), collagen alpha-1(I) chain (*COL1A1*), and small leucine-rich proteoglycans, like lumican (*LUM*), decorin (*DCN*) and biglycan (*BGN*) genes [5]. The altered secretory function of transdifferentiated SMCs [7] modifies ECM composition, by replacing type I and III fibrillar collagens [7] with fibronectin and proteoglycans, and contributes to vascular remodeling and lesion development. These ECM changes also influence lipid accumulation and cellular proliferative index. In addition to the fibroblast-like phenotype, SMCs can in fact acquire macrophage- and osteo/chondrogenic-like phenotypes after phenotypic switch [9,10] and take up and store excess lipids forming foam cells [8].

Cigarette smoke may induce SMC phenotypic switch [11] and is recognized as one of the most important modifiable risk factors for cardiovascular diseases (CVDs) [12]. Traditional tobacco cigarette (TC) smoke is constituted of approximately 7000 different components, with lipophilic or water-soluble properties, that are distributed between particulate matter and gas phases. Many of these chemicals are known to be antigenic, cytotoxic, mutagenic, or carcinogenic [13]. As alternatives, electronic cigarettes (E-cigs) and tobacco heating products (THPs) have been marketed as safer options, though evidence supporting these claims remains limited, particularly regarding long-term CV effects [14]. E-cigs use a battery-supplied electric current to heat (at 200–250 °C) a liquid mixture typically composed of propylene glycol, vegetable glycerin, nicotine, and different types of flavors, but generate toxic compounds such as heavy metals (nickel, cadmium, chromium) and carbonyls (*i.e.* formaldehyde, acetaldehyde, acrolein) [15]. In addition, flavorings contain alcohol, aldehydes, and chemicals such as diacetyl and acetylpropionyl, commonly used by food manufacturers but that can cause lung damage when inhaled [16]. Increasing evidence of CV effects, including endothelial cell dysfunction, oxidative stress, arterial stiffness, and acute alterations in heart rate and diastolic blood pressure, highlight the potential for E-cigs to contribute to CVDs [17–21]. On the other hand, THPs heat (at 350 °C) sticks of compressed tobacco, flavors, and other chemicals to produce a nicotine aerosol [22], thus avoiding the combustion phase typical of TC. Nonetheless, although THPs produce fewer toxicants than TCs, they still adversely affect the CV system by increasing arterial stiffness [23] and oxidative stress [24]. Therefore, despite their reduced impact compared to TCs, the effects of E-cigs and THPs on CV health are not negligible.

Building on our prior findings regarding SMC exposure to lipophilic TC smoke condensate components [11], this *in vitro* study explored the impact of aqueous extracts (AEs), containing water-soluble components, from TC, E-cig, and THP smoke on human aortic SMC phenotypic modulation, with potential implications for CV health and atherosclerosis progression.

2. Materials and Methods

Detailed Materials and methods are available in the "Materials and Methods" section of the Supplementary Material.

2.1. Human aortic smooth muscle cell culture

Human aortic SMCs (HASMC; PCS-100-012) were purchased from ATCC (Manassas, FL, USA), and cultured in ATCC Vascular Cell Basal Medium (PCS-100-030, ATCC; 500 ml added with 500 µl ascorbic acid, 500 µl rh EGF, 500 µl rh insulin and rh FGF-b, 25 ml glutamine), 5 % fetal bovine serum (FBS, ATCC Vascular Smooth Muscle Growth Kit), and 5 ml Penicillin-Streptomycin 100X (Euroclone, Milan, Italy). The cultures were maintained at 37 °C in a 5 % CO_2 incubator. All the experiments were performed with HASMC between passages 5–9.

TC, E-cig and THP extracts Generation.

The aqueous extracts (AEs) used in this study were kindly provided by British American Tobacco Ltd., (Southampton, UK) and prepared as described [25].

For AEs from TC, we used a Kentucky Reference cigarette (1R6F) as a scientific reference comparator for mainstream smoke (Kentucky Tobacco Research & Development Center, Lexington, USA; for THP we used one THP device (Glo™); and for E-cig, a distiller plate technology format (Vype iSwitch).

2.1.1. Proteomics and interactomics analyses

Relative quantitative Mass Spectrometry (MS) analysis was performed through Label Free Quantification (LFQ). For statistical comparisons, nonparametric statistics was applied (p-value $\leq$0.05; minimal fold change (FC) of $\pm$1.5). Significant transcript and protein differences were functionally correlated in interactomic networks to recognized highly significant biomarkers for several health applications, as we previously proved [26–29].

2.2. Statistical analysis

GraphPad Prism 10 was used for statistical analysis. All experiments were repeated at least three times in triplicates using different batches of AEs. For multiple comparisons testing, 1-way ANOVA accompanied by a Dunnett's post hoc test were used as appropriate. All error bars represent standard error of the mean. A probability value of $p < 0.05$ was considered statistically significant.

Non-common abbreviations used in the text.

AE = aqueous extract.
CSC = cigarette smoke condensate.
E-cig = electronic cigarette.
HASMC = human aortic SMC.
TC = traditional cigarette.
THP = tobacco heating product.

3. Results

3.1. TC, E-cig, or THP AEs induce phenotypic changes in cultured HASMCs

We analyzed the effects of smoke from tobacco-derived product on SMC by exposing HASMCs to TC, E-cig, and THP AEs for 48h. The AE concentration to be used was determined based on preliminary cytotoxicity experiments. The concentration that was found to be non-toxic for all extracts was 10 % (Supplementary Figure S1) and it was used in all the following experiments. Firstly, we evaluated AE-induced phenotypic modulation by investigating the expression of HASMC contractile markers, ECM components, MMPs, proinflammatory genes, and macrophage-specific markers. Subsequently, to further elucidate the effects of AEs on HASMC phenotypic modulation, we measured the ability of AEs to influence cell proliferation, migration, and cytoskeletal organization.

3.1.1. AE effects on the expression and synthesis of ECM-components and of contractile, macrophage-specific, and inflammatory markers

As shown in Fig. 1A, the treatment with all three extracts led to an upregulation of a key contractile gene *ACTA2* (encoding smooth muscle alpha-actin). The E-cig AE was the most potent, significantly enhancing *ACTA2* expression by approximately 2.7-fold. THP AE elevated *ACTA2* expression by 50 % compared to control and TC AE. These gene expression changes were reflected at the protein level, as evidenced by increased *ACTA2* protein levels upon exposure to THP and E-cig AEs.

The transcription factor Krüppel-like factor 4 (KLF4) and Myocardin (MYOCD) axis play a crucial role in SMC modulation [1]. KLF4 is a key regulator of SMC phenotypic modulation, where it suppresses the expression of SMC-specific contractile genes such as *MYOCD* and *ACTA2* [2]. Therefore, we quantified the expression and protein levels of *MYOCD* and *KLF4* in HASMCs. As shown in Fig. 1B, the addition of the

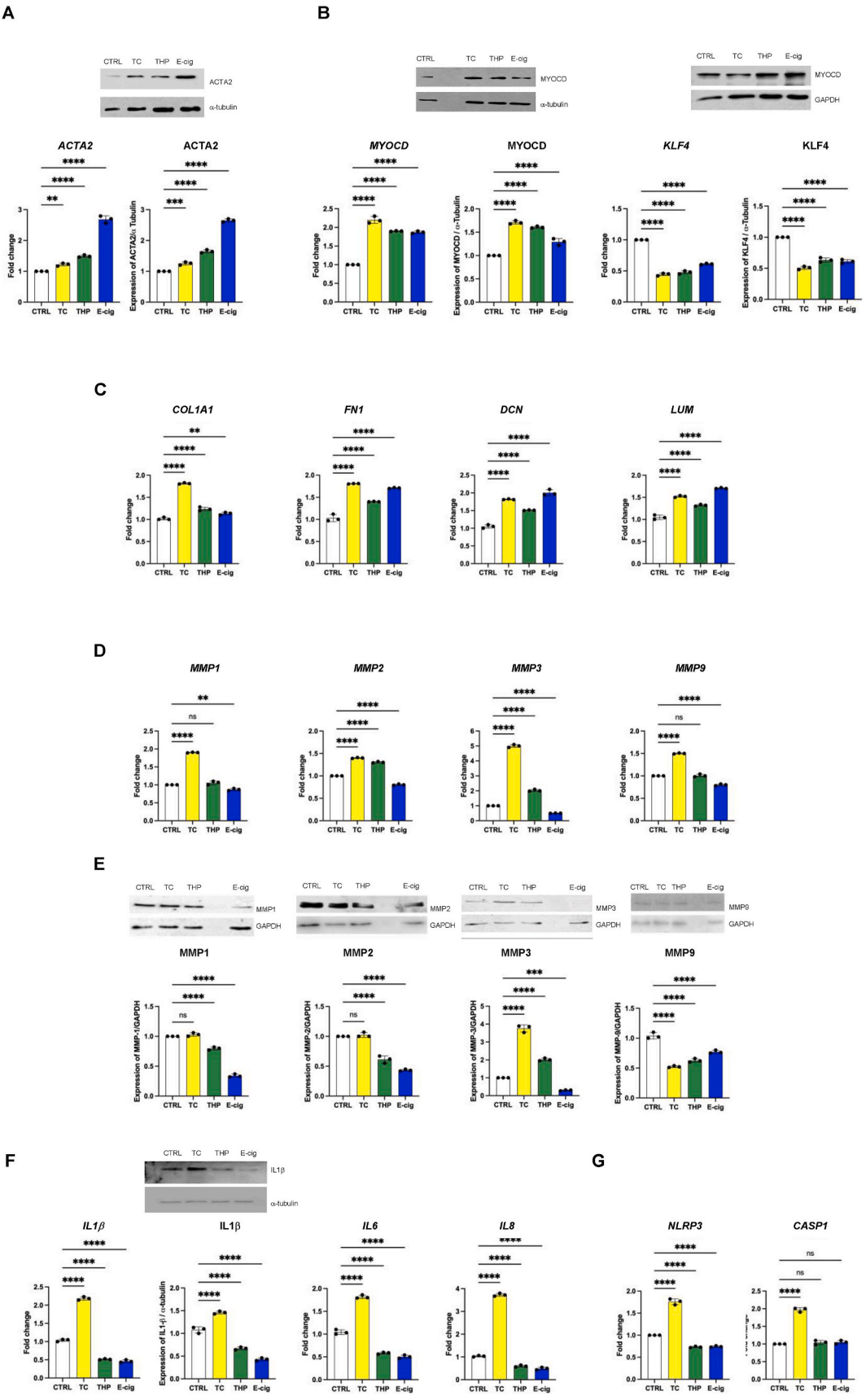

Fig. 1. TC, E-cig and THP AEs induce phenotypic switching in HASMCs. HASMCs were treated with 10 % AEs for 48h. Then we evaluated: **(A)** SMC-specific contractile, (**B**) phenotypic, and (**C**) ECM markers, (**D** and **E**) MMP, (**F**) interleukin, (**G**) inflammasome marker gene expression and protein abundance, (**H**) HASMC proliferation, (**I**) PCNA gene expression and protein abundance. Gene expression was evaluated by RT-PCR and protein abundance (normalized by indicated housekeeping proteins) by western blot analysis. (**J**) HASMC migration was assessed by wound healing assay and images were taken 0,4, 8, 10, 20 h after wounding.

(**K**) Quantification of the migrated cells was then performed with ImageJ. Scale bar: 200 μm. (L) F-actin expression was evaluated by confocal microscopy. (**M**) *RAC1* expression and protein abundance were measured by RT-PCR or western blot analysis, respectively. Each result displayed is representative of at least 3 independent biological replicates. The p-value was determined by one-way ANOVA followed by Dunnett post hoc test * $p < 0.05$ vs CTRL, **$p < 0.01$ vs CTRL, ***$p < 0.001$ vs CTRL, ****$p < 0.0001$ vs CTRL.

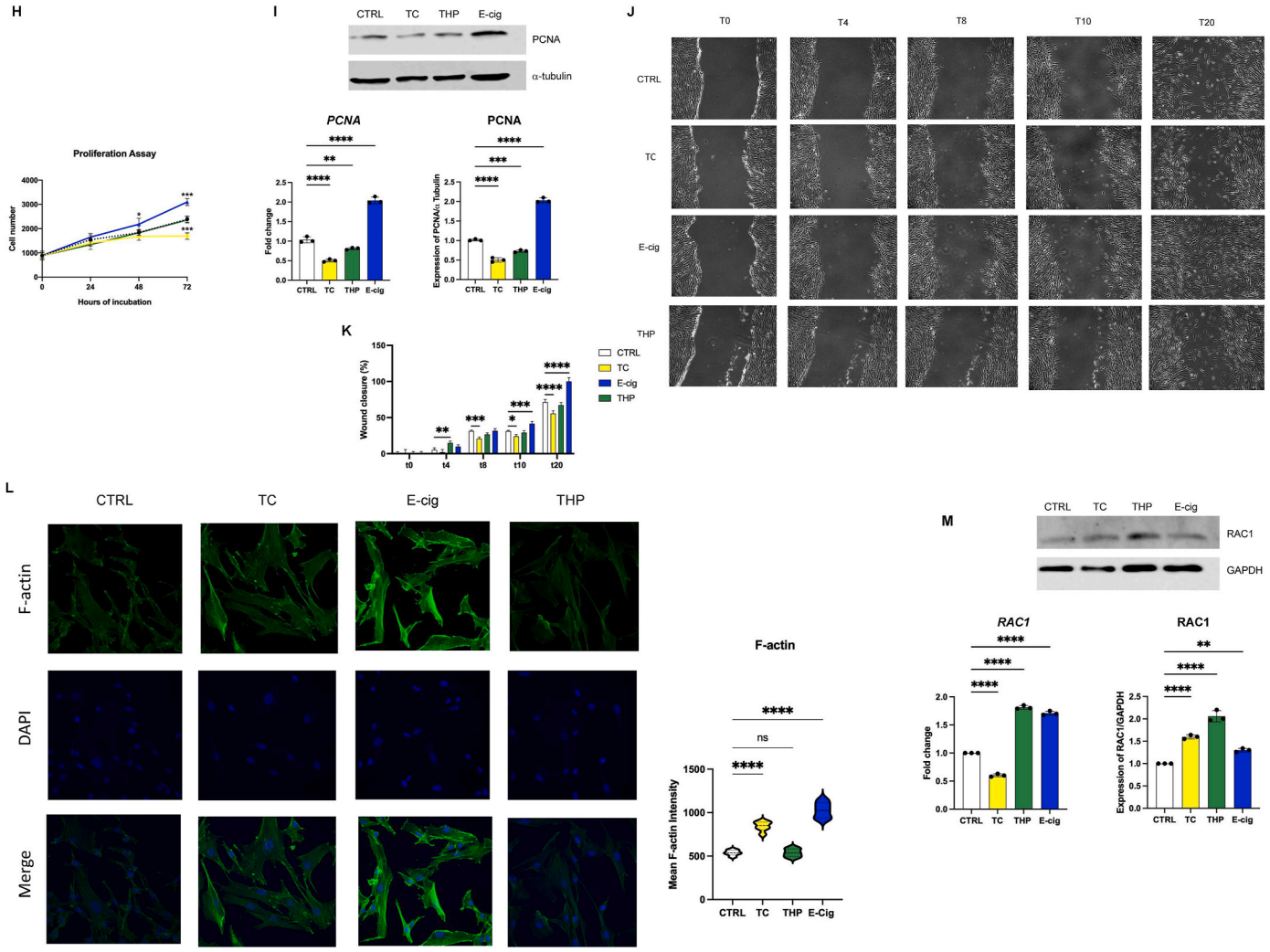

Fig. 1. (*continued*).

three extracts increased the expression of *MYOCD*, while concurrently reducing KLF4 at both gene and protein levels.

Additionally, we assessed the effects of AEs on ECM markers. As shown in Fig. 1C, all three AEs led to a significant upregulation of *COL1A1*, *FN1*, *DCN*, and *LUM* expression indicating an impact on ECM remodeling.

Furthermore, the exposure to TC AE led to an upregulation of *MMP* expressions (interstitial collagenase *MMP1* by almost 2-fold, collagenases *MMP2* and *MMP9* up to 1.5-fold, and stromelysin-1 *MMP3* 5-fold; Fig. 1D). Conversely, THP AE upregulated *MMP2* and *MMP3* (by 1.3-fold and 2-fold, respectively) but did not affect the expression of *MMP1* or *MMP9*. In contrast, E-cig AE slightly reduced the expression of *MMP1*, *MMP2*, and *MMP9*, while halved the expression of *MMP3* (Fig. 1D). By western blot analyses, we also investigated the effects of AEs on MMP protein levels. TC AE increased MMP3 levels by 4-fold, did not affect MMP1 and MMP2, and halved MMP9 abundance (Fig. 1E). THP AE decreased MMP1, MMP2, and MMP9 presence, while it doubled the amount of MMP3. In contrast, E-cig reduced the presence of all the MMPs evaluated, especially MMP3 (up to 80 % decrease; Fig. 1E).

Exposure to TC AE greatly increased the expression of the proinflammatory markers interleukin-1β (*IL1B*), interleukin-6 (*IL6*), and interleukin-8 (*CXCL8* or *IL8*) (up to more than 3-fold for the latter; Fig. 1F) as well as that of the genes encoding NACHT, LRR, and PYD domains-containing protein 3 (*NLRP3*) and Caspase-1 (*CASP1*) (by 1.8-fold and 2-fold, respectively) (Fig. 1G). Conversely, the same markers were either reduced by half (Fig. 1F) or partially reduced (Fig. 1G) in cells incubated with E-cig and THP AEs. *CASP1* was unaffected by E-cig and THP AEs (Fig. 1G). Modulation of IL-1β protein levels were confirmed by western blot analysis (Fig. 1F insert).

Previously, we showed that cigarette smoke condensate (CSC) induces a phenotypic switch in SMCs by reducing the expression of contractile markers and increasing the expression of macrophage markers LGALS3 and CD68 [11]. However, in the present study, some AEs increased the expression of contractile markers and did not affect the expression of the macrophage markers *LGALS3* and *CD68* (Supplementary Figure S2).

3.1.2. *Proliferation and migration in AE-treated HASMCs*

The AE capability to stimulate HASMC proliferation was tested by cell counting at different time-points of incubations with AEs (Fig. 1H), and by measuring gene expression and protein abundance of the proliferating cell nuclear antigen (*PCNA*) (Fig. 1I), a key factor in DNA

replication and cell cycle regulation [30].

E-cig AE significantly stimulated HASMC proliferation (Fig. 1H). This effect was already evident after 48 h of treatment and further enhanced after 72 h. In contrast, the addition of TC AE slowed the HASMC proliferative rate, especially after 72 h when cells stopped growing, while THP extract did not affect HASMC proliferation (Fig. 1H). The abundances of *PCNA* mRNA and the corresponding coded protein confirmed these data. E-cig AE doubled *PCNA* expression, while TC AE halved it. THP AE only slightly affected *PCNA* at both gene and protein levels (Fig. 1I).

The capacity of AEs to stimulate HASMC migration was then assessed by measuring cell directional migration. Notably, E-cig AE was the most effective in inducing a faster wound re-closure by leading to an almost complete healing of the lesioned area after 20 h (Fig. 1J and K). On the contrary, the addition of TC extract inhibited HASMC migration, while THP AE did not affect wound reclosure rate (Fig. 1J and K). These results were confirmed by using a transwell chemotaxis assay. Treatment with E-cig AE significantly enhanced HASMC migration by 60 %. In contrast, TC AE reduced the number of migrated cells by 10 %, and THP AE did not have any effect (Supplementary Figure S3).

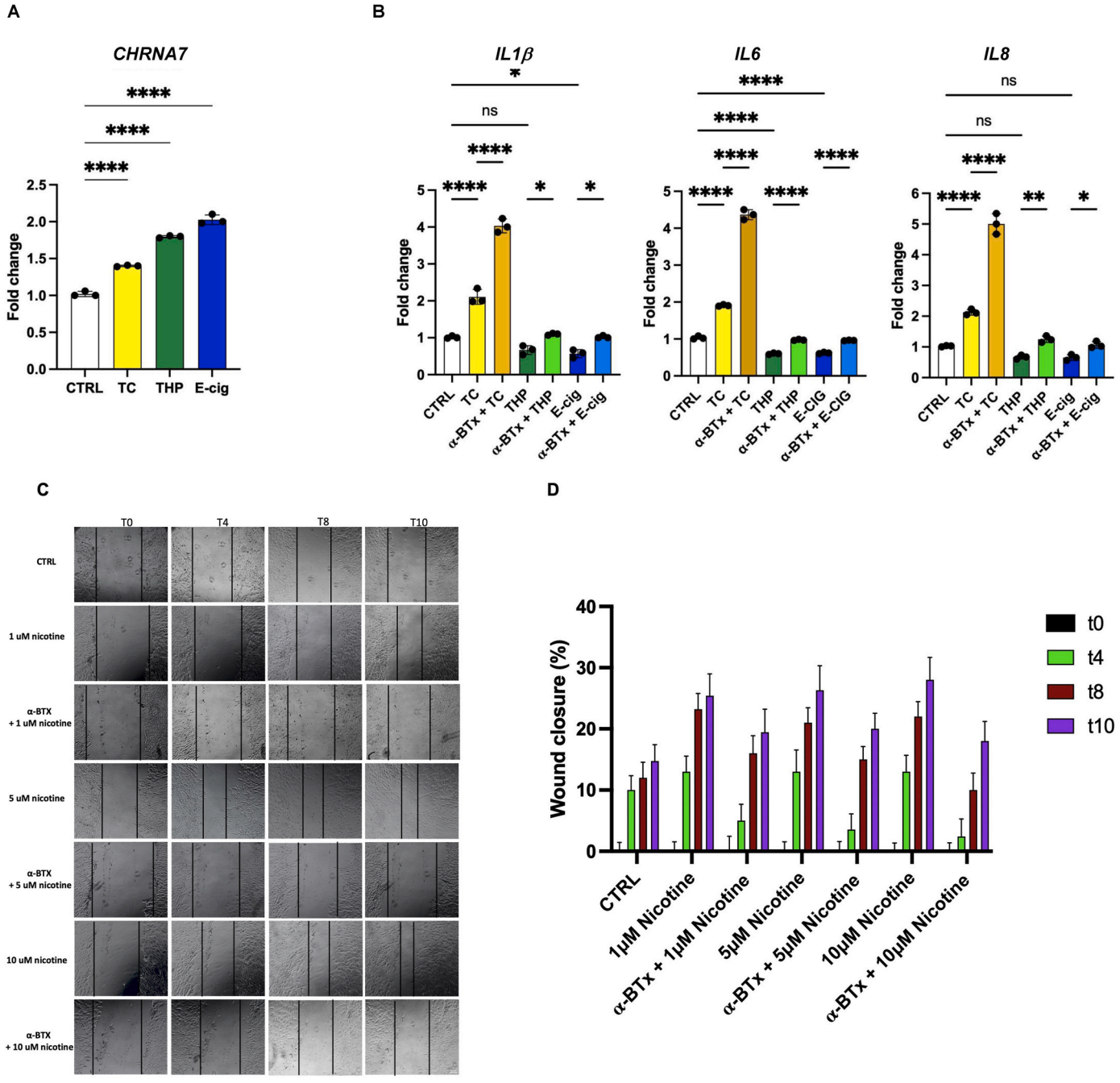

Fig. 2. AEs affect the expression of inflammatory markers and nicotine induces HASMC migration through the CHRNA7. HASMCs were treated with 10 % AEs for 48h. RNA was extracted, and gene expression evaluated by RT-PCR. **(A)** *CHRNA7* and **(B)** *IL-1β, IL-6* and *IL-8* gene expression in presence or in absence of α-BTX. **(C)** Cell migration capability was assessed by wound healing assay and images were taken 0,4, 8, 10 h after wounding. **(D)** Quantification of the migrated cells was then performed with ImageJ. Scale bar, 200 μm. Each result displayed is representative of at least 3 independent biological replicates. The p-value was determined by one-way ANOVA followed by Tukey's post hoc test and considered significant for * $p < 0.05$ vs CTRL * $p < 0.05$ vs **α**-BTx + E-cig, *$p < 0.05$ vs **α**-BTx + THP, **$p < 0.01$ vs **α**-BTx + THP, ****$p < 0.0001$ vs CTRL, ****$p < 0.0001$ vs **α**-BTx + TC, ****$p < 0.0001$ vs **α**-BTx + E-cig, ****$p < 0.0001$ vs **α**-BTx + THP.

Cell migration is initiated by actin-dependent protrusions of lamellipodia and filopodia [31]. Therefore, to further elucidate the effects of tested-smoke extracts, we investigated HASMC cytoskeleton organization in response to AE exposure. As shown in Fig. 1L, phalloidin staining revealed differences in fluorescence intensity (FI) of filamentous actin (F-actin) after AE incubation. E-cig AE exhibited the strongest effect, leading to a 2-fold increase in FI. In contrast, TC AE caused a modest increase of FI, while THP AE did not significantly modify it.

Since the regulation of actin dynamics in SMCs is critically mediated by the Rho family of small GTPases, particularly by RAC1, which facilitates F-actin polymerization through Arp2/3-complex activation [32], we assessed the impact of AEs on RAC1. E-cig AE significantly upregulated *RAC1* expression and protein abundance by 1.7-fold and 1.3-fold, respectively (Fig. 1M). On the other hand, TC AE reduced *RAC1* expression (by 40 %) but enhanced its protein level (by 60 %). Notably, THP AE resulted in a marked upregulation of both *RAC1* expression and protein levels (by 1.8-fold and 2.2-fold, respectively).

3.2. The neuronal acetylcholine receptor subunit alpha-7 mediates E-cig and THP AE-induced anti-inflammatory pathway activation in HASMCs

The activation of neuronal acetylcholine receptor subunit alpha-7 (CHRNA7), also named cholinergic receptor nicotinic alpha 7 subunit, exerts anti-inflammatory and immune modulatory reactions [33]. Thus, we investigated whether the AEs affected the inflammatory pathways *via* CHRNA7 stimulation.

First, we proved that all the tested AEs significantly increased the expression of *CHRNA7*: E-cig AE doubled it, while THP and TC AEs upregulated its expression by 1.8- and 1.4-fold, respectively (Fig. 2A). Next, HASMCs were pretreated for 30 min with α-BTX (1 μM), a potent antagonist of CHRNA7. Pretreated cells were then exposed to AEs for 48 h and *IL1B*, *IL6*, and *IL8* expression was measured by real-time PCR. α-BTX effectively reversed the inhibitory effects induced by E-cig and THP AE treatments and further amplified the stimulatory effect of TC AE on interleukin gene expression (Fig. 2B).

3.2.1. Nicotine promotes HASMC migration via the activation of CHRNA7 receptor

One common component of all the tested AEs is nicotine, although its concentration differs in the three extracts: 4.3 μM in TC, 6.1 μM in E-cig, and 8.6 μM in THP. Nicotine promotes SMC migration *via* nicotinic acetylcholine receptors (nAChRs) and G protein-coupled receptors [34,35]. Therefore, to investigate if the different results observed after AE treatments were related to the different nicotine contents, we tested the effects of nicotine alone on HASMC migration. As shown in Fig. 2C–D, nicotine stimulated cell migration. Almost 30 % of the wounded area was healed after 10 h exposure to 10 μM nicotine, versus only a 15 % recovery observed in the control group. Monolayer wounds were completely healed after 20 h of treatment.

To further clarify the role of CHRNA7 in nicotine-induced cell migration, α-BTX 1 μM was added to the culture media 30 min before nicotine exposure. α-BTX reduced nicotine-induced cell migration at all the tested nicotine concentrations: by 6 % at nicotine concentrations of 1–5 μM and by 10 % at 10 μM (Fig. 2D).

In conclusion, the nicotine content in the AEs may, at least in part, promote HASMC migration *via* the activation of CHRNA7.

3.3. Integrated interactomics of HASMCs exposed to TC, E-cig, and THP AEs

A label-free quantitative proteomics analysis identified 10 differentially abundant proteins that significantly (FC $\geq$ 1.5, $p \leq 0.05$) characterized control cells and HASMCs exposed to TC, E-cig, and THP AEs (Table 1 and Supplementary Table S2).

The variance-covariance analysis was performed by principal component analysis (PCA) on abundance values of significantly differing proteins identified by MS. The first three axes of variation, *i.e.*, PC1, PC2, and PC3, explain the 62.5 %, 30.6 %, and 6.9 % of the variance, respectively. The PC1/PC2 plot shows control cells and TC AE-treated HASMCs clustering apart from cells exposed to THP and E-cig AEs, which localize on the right side of PC1 (Fig. 3A). Controls and TC AE-treated HASMCs separate mainly in reason of PC2. All the tested conditions present a very low intra-class variability, as highlighted by signal overlapping of biological replica in each sample class (Fig. 3A–B).

Table 1
Differentially abundant proteins identified among control and AE-treated cells.

Gene name (synonym)	Protein name	UniProtKB AN	MetaCore name
AP1M1 (CLTNM)	AP-1 complex subunit mu-1	Q9BXS5	AP1M1
COX4I1 (COX4)	Cytochrome *c* oxidase subunit 4 isoform 1, mitochondrial	P13073	COX IV-1
EFEMP1 (FBLN3, FBNL)	EGF-containing fibulin-like extracellular matrix protein 1	Q12805	Fibulin-3
HMOX1 (HO, HO1)	Heme oxygenase 1	P09601	Heme oxygenase 1
IDH3A	Isocitrate dehydrogenase [NAD] subunit alpha, mitochondrial	P50213	IDH3A
MGEA5 (HEXC, KIAA06791, MEA5, MGEA5)	Protein O-GlcNAcase	O60502	MGEA5 (GLCNACase)
PROCR (EPCR)	Endothelial protein C receptor	Q9UNN8	ROCK2
ROCK2 (KIAA0619)	Rho-associated protein kinase 2	O75116	Protein C receptor (endothelial)
SOD2	Superoxide dismutase [Mn], mitochondrial	P04179	SOD2
UBE2I (UBC9, UBCE9)	SUMO-conjugating enzyme UBC9	P63279	E2I

The heatmap shows the relative abundances of the 10 identified differences clustered according to their similarity, as evidenced by the vertical dendrogram (Fig. 3C). Analogously to PCA, the heatmap suggests interesting similar protein profiles between control and TC AE-exposed cells and between E-cig and THP AEs. Variance-contribution of individual proteins (heatmap rows) to the three main principal components is displayed by the matrix interposed between the vertical dendrogram and the heatmap.

To comprehensively evaluate their functional relevance in the investigated four conditions, MS/MS-identified protein differences were combined with WB-detected differentially abundant proteins. The resulting 20 experimental differences were co-processed by applying direct interaction algorithm (DIA) from the MetaCore network building tool. The obtained network includes all the analyzed proteins, except for endothelial protein C receptor (PROCR) (Fig. 3D). This proves the high biological relevance of the investigated proteins since only factors showing functional direct interactions enter into the net. As a result, the latter represents the biochemical core of treatment-induced effects in HASMCs. KLF4, MMP2, MMP9, IL1B (IL1 beta in MetaCore), and EGF-containing fibulin-like extracellular matrix protein 1 (EFEMP1; fibulin-3 in MetaCore) are the main nodes, with individual relevance corresponding to the order in which they are listed.

The DIN trace mode visualization centered on the five central hubs properly visualizes the tight functional interconnection existing among them (Fig. 3E). MMP2 and MMP9 directly interact with the other four central hubs, while EFEMP1 directly interacts only with MMP2 and MMP9. KLF4 and IL1B do not directly interact with EFEMP1, but the former uses MMP2 and MMP9, and the latter MMP3 (Stromelysin-1 in MetaCore), as molecular bridges for functional correlation to that ECM protein.

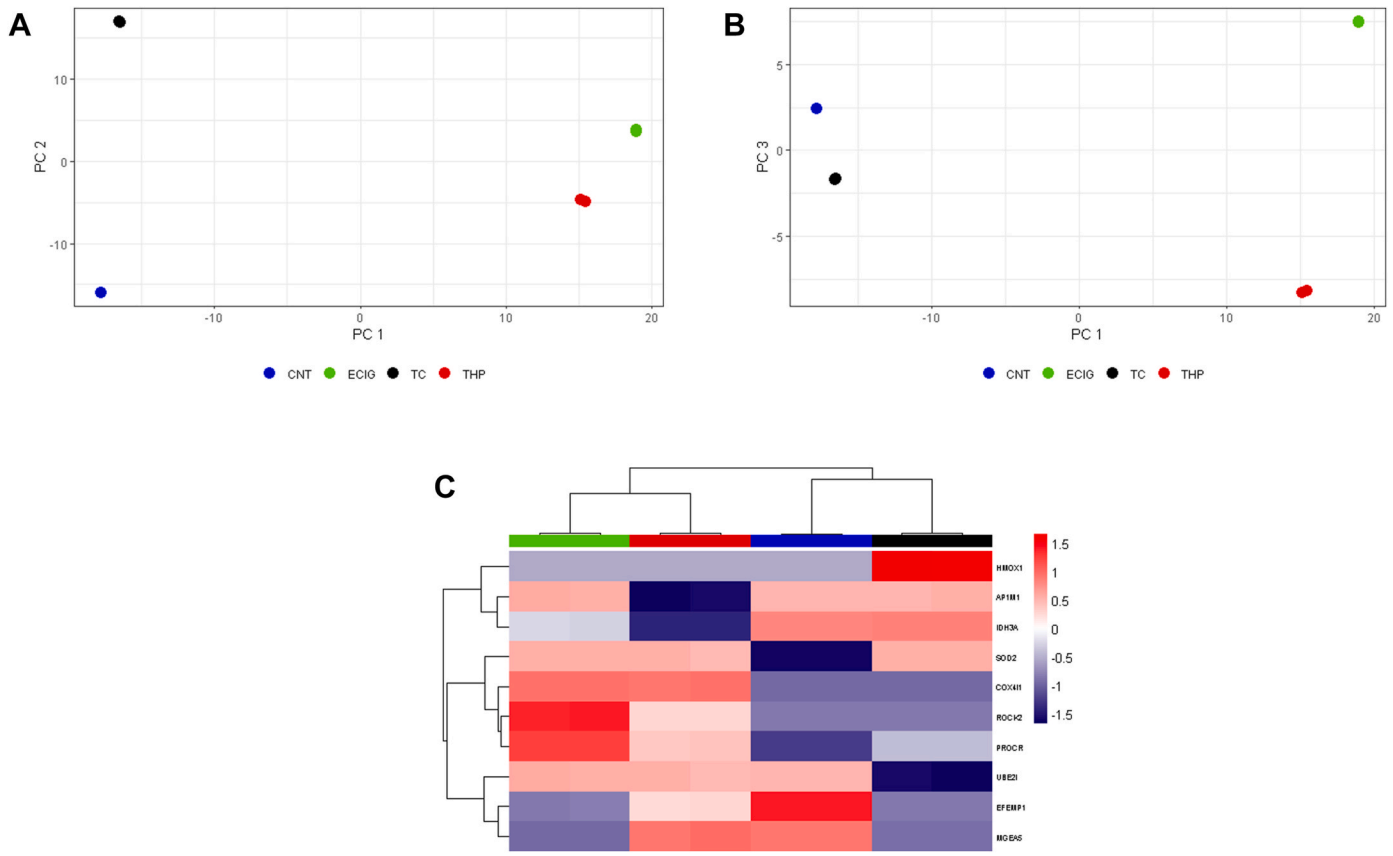

Fig. 3. Proteomic analysis and interaction networks of AE effects on HASMCs. (A) (B) Principal component analysis (PCA) performed on abundance values of the 10 protein differences obtained from the MS differential analysis. The plots highlight spatial distribution of the investigated samples [from control cells (blue symbols), TC (black symbols), THP (red symbol), and E-cig (green symbols)] in reason of their variance combined in the three main components: PC1/PC2 (A) and PC1/PC3 (B). **(C)** Heatmap representing Euclidean distances of abundance values from the 10 MS identified/quantified protein differences – horizontal bars: blue = control cluster; black = TC cluster; green = E-cig cluster; red = THP cluster. (**D**) Protein direct interaction network built by co-processing MS identified differences and differentially abundant proteins detected by WB. (**E**) Trace mode visualization of the protein-DIN highlighting the tight functional crosstalk among the 5 central hubs. (**F**) Gene-protein hybrid direct interaction network built by co-processing differentially expressed genes and differentially abundant proteins detected in SMCs exposed to AEs. (**G**) Trace mode visualization of the gene-protein-DIN highlighting the tight functional crosstalk among the 4 metalloproteinases. (**D**–**G**) Edge colors and arrowheads indicate the type and direction of protein interconnections. Green arrows indicate positive effects, red ones negative effects, and the grey arrows indicate unspecified interactions. (For interpretation of the references to color in this figure legend, the reader is referred to the Web version of this article.)

Successively, to amplify the understanding of the biological effects of AE treatments on HASMCs, we performed an interactomic evaluation of the deregulated genes, detected by RT-PCR, by combining them with the above-described 20 protein differences (from MS and WB analyses). According to the MetaCore DIA, we generated a gene-protein hybrid network (Fig. 3F) where only PROCR and LUM did not enter. Here, the first three principal nodes from the protein-DIN, i.e. KLF4, MMP2, and MMP9, are maintained as central hubs, while IL1B and EFEMP1 are replaced by MMP1 and MMP3, respectively.

Both protein and gene-protein networks confirm a critical role played by KLF4 in HASMCs after smoke extract treatments, as we previously proposed [11]. This node established the highest number of interactions with the majority of the processed experimental factors, which were modulated in both presence or expression by exposure to AEs. In addition, the protein-gene hybrid network is centered on MMPs, which are correlated by reciprocal induction and that converge, directly or indirectly, on MMP9, as stressed by the focalized trace mode visualization (Fig. 3G).

4. Discussion

AEs from TC, E-cig, and THP constitute 90–95 % of cigarette smoke mass (gas and particulate matter), mimicking *in vivo* exposure by capturing water-soluble components [25,36,37]. Our study evaluated their effects on HASMC phenotypic switch, a key process in atherosclerosis [1]. TC AE induced a pro-inflammatory and pro-degradative environment, while E-cig AE suppressed the inflammatory response but increased cell proliferation and migration. THP AE showed intermediate effects.

AEs upregulated the contractile gene *ACTA2* without inducing macrophage markers (*LGALS3*, *CD68*) typical of CSC exposure [11], suggesting distinct effects of AEs on SMC behavior. They also upregulated *MYOCD*, a key transcriptional regulator of SMC contractility, and reduced the expression of *KLF4*, a repressor of *MYOCD* and promoter of SMC phenotypic switching [38,39]. Despite strengthened contractile phenotype may stabilize plaques [40], elevated *ACTA2* expression can drive SMC osteogenic differentiation and aorta calcification [41].

All the investigated AEs upregulated ECM-related genes (*COL1A1*, *FN1*, *DCN*, *LUM*) and HASMCs exposed to them may adopt a dual contractile-synthetic phenotype, indicative of an intermediate SMC state [42]. The upregulation of ECM compounds may stabilize the plaque by reinforcing its fibrous cap, but it could also promote fibrosis, furthering plaque progression or reducing vessel dilation. E-cig use has been linked to reduced microvascular function in young adults [43].

Our study highlighted also differential inductions in HASMCs depending on the tested AE. TC AE induced a pro-degradative

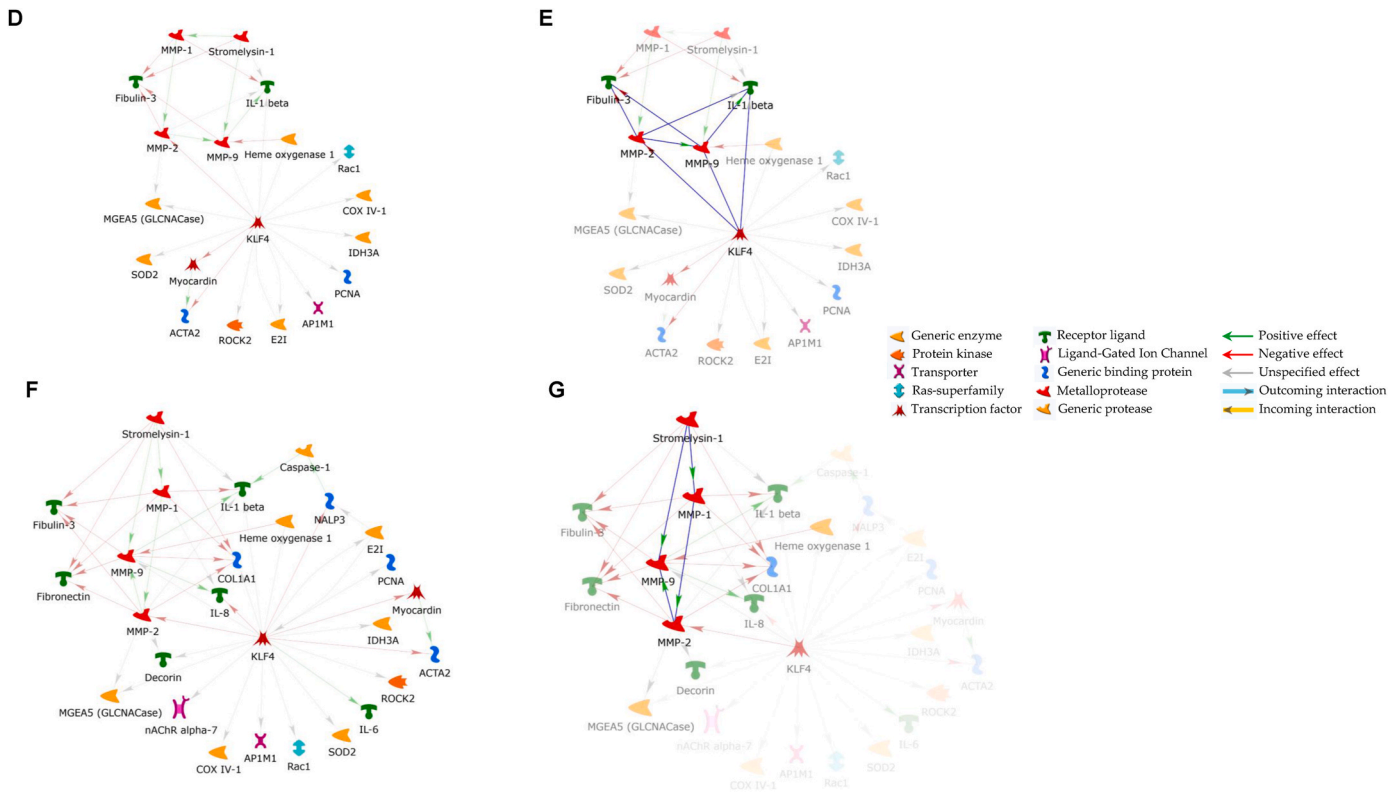

Fig. 3. (*continued*).

environment, elevating *MMP1*, *MMP2*, *MMP3*, and *MMP9* gene expression and MMP3 protein levels, potentially weakening plaque integrity. THP AE increased *MMP2* and *MMP3* transcription similarly, but reduced most MMPs, except for MMP3 that significantly increased. Conversely, E-cig AE may mitigate ECM degradation and plaque rupture by reducing MMP gene expression and protein concentration, particularly of MMP3. Moreover, since MMP3 is upregulated in SMC osteogenic transformation and plays a critical role in SMC calcification [44] and vessel stiffness, the downregulation of this protein may reduce plaque calcification risk and vessel rupture in E-cig smokers. Nonetheless, the long-term MMP suppression may favor fibrosis and vessel stiffening, a process implicated in vascular SMC aging and atherosclerosis development [45].

A potential link between TC AE and osteogenic-like switching in HASMCs is further suggested by decreased O-GlcNAcase (OGA) levels in TC-treated cells. OGA is a key enzyme in controlling protein O-GlcNAcylation, whose increase promotes pro-atherosclerotic gene expression (e.g. *TSP-1*, *TGF-β*, *PAI-1* and *NF-kB)* [46]. Elevated O-GlcNAc is associated with vascular calcification in diabetes, and OGA inhibition causes vascular SMC calcification *in vitro* [47]. Interestingly, we detected decreased OGA abundance also in E-cig AE exposed cells.

Furthermore, mitochondrion dysfunction impairs redox homeostasis thus further contributing to SMC osteoblastic-like phenotype-switch and related calcification [47]. Our MS-proteomic analysis recognized differential abundances of cytochrome *c* oxidase subunit IV isoform 1 (COX4I1) and of isocitrate dehydrogenase [NAD] subunit alpha (IDH3A), both implied in the control of the mitochondrion energy flow. While IDH3A decreased, COX4I1 increased in both E-cig and THP AE-treated cells. The IDH3A reduced abundance, principally in THP AE-exposed cells, may lead to a decreased production of the antioxidant α-ketoglutarate [48], and of NADH, harnessed into ATP, via the electron transport chain, or converted to NADPH, by the nicotinamide nucleotide transhydrogenase [49]. NADPH is a key antioxidant molecule via the glutathione and thioredoxin reductase enzymes [49] and through the heme oxygenase 1 (HMOX1), which we detected widely increased in TC AE-treated HASMCs. In spite its role in redox balancing, HMOX1 increases iron content, ROS, and lipid peroxidation in diabetic endothelial cells, and it may even trigger ferroptosis in diabetic atherosclerosis development [50]. Reduced α-ketoglutarate may impair α-ketoglutarate-dependent dioxygenases, such as the prolyl hydroxylases PHD1-3, which inhibit hypoxia-inducible factor (HIF)-1, and prolyl-3 and prolyl-4 hydroxylases (P3H, P4H) [51]. Since HIF-1α drives SMC osteochondrogenic differentiation [52], and collagen prolyl-hydroxylation is essential for functional collagen and physiological ECM biosynthesis, the possible E-cig and THP AE-dependent α-ketoglutarate diminution may participate to calcification and reduced stability of atherosclerotic lesions *in vivo*.

Additionally, mitochondrial manganese superoxide dismutase [Mn] (SOD2) levels increased in all the AE-treated HASMCs. The increase of COX4I1, a component of the electron transport chain complex IV that couples the rate of ATP production to energetic requirements and that controls COX oxygen affinity [53], may correlate, when combined with a possible NADH depletion and a consequent electron leakage, with incomplete reduction of molecular oxygen and ROS generation. Overall, each AE affects distinct panels of molecular steps or processes involved in the regulation of mitochondrion activity and cellular redox state.

Inflammatory responses varied by AE type. TC AE increased *IL1B*, *IL6* and *IL8* expression, and IL1B protein presence, indicating a pro-atherogenic inflammatory profile linked to immune recruitment and plaque formation, development and instability [54,55]. In contrast, E-cig and THP AEs reduced the expression of pro-inflammatory cytokine genes and induced an anti-inflammatory response via the upregulation of *CHRNA7*, upregulated also in TC AE-exposed cells. Pharmacological inhibition of CHRNA7, by its antagonist α-BTX, confirmed its role in mitigating AE-induced inflammation, suggesting a potential counter-regulatory response, with the most proportionally pronounced effect triggered by TC AE. AEs from both devices, in particular from E-cig, raised ROCK2 abundance. This is a critical regulator of endothelial inflammation and immune cell recruitment, whose activation in SMCs

contributes to phenotype switching, increased proliferation and migration, and vascular remodeling and stiffening [56–60]. Therefore, despite some anti-inflammatory signaling, our data suggest, once more, that these devices may have detrimental pro-inflammatory and pro-fibrotic consequences inducing adverse vascular remodeling.

There is growing interest in understanding how newer nicotine delivery products, like E-cig and THP, compare with TCs. Nicotine, common to all AEs, enhanced HASMC migration in a CHRNA7-dependent manner, as shown before [61]. E-cig AE significantly enhanced HASMC proliferation, with a marked increase in the expression and protein levels of PCNA [30], whereas TC AE significantly reduced proliferation, halving *PCNA* expression and protein abundance. Consistently others showed E-cig vapor promotes cellular proliferation and cell cycle progression [62,63], whereas TC smoke tends to inhibit such processes by inducing apoptosis and DNA damage [64,65]. Furthermore, the wound healing assay demonstrated that E-cig AE significantly accelerated HASMC migration, while TC AE inhibited migration and THP AE had no significant effect. On the same line, TC extract decreases endothelial cell migration rate [66].

Additionally, we assessed F-actin and *RAC1*, a key mediator of cytoskeletal reorganization and cell migration [67] often associated with ROCK2. Variations in ROCK2 levels may account for the differential proliferation and migration behavior of AE-treated HASMCs. E-cig AE led to a 2-fold increase in F-actin and upregulated both *RAC1* gene expression and protein levels, possibly through actin polymerization and cytoskeletal reorganization. Conversely, TC AE modestly increased F-actin levels and reduced *RAC1* expression, but it enhanced RAC1 protein abundance, hence indicating a complex regulation of RAC1 in response to TC extract. THP AE also upregulated *RAC1* expression and its protein abundance, although to a lesser degree than E-cig AE. RAC1 regulates actin cytoskeleton dynamics, promoting lamellipodia formation and cell migration, particularly in response to nicotine [68]. The differential effects of E-cig, TC, and THP extracts on RAC1 and F-actin highlighted the distinct cellular mechanisms underlying the migration and proliferation of HASMCs, which are likely driven by nicotine concentration and other smoke constituents. These findings raise important questions about the long-term CV risks of E-cigs and other nicotine delivery products, as the enhanced proliferation and migration of SMCs could contribute to the development of vascular dysfunctions. While THP AE had minimal effects in comparison to E-cig and TC AEs, the upregulation of RAC1 suggests that it may still pose a risk by promoting vascular remodeling.

Proteomics analysis detected reduction of EGF-containing fibulin-like extracellular matrix protein 1 (EFEMP1 or fibulin-3), which is linked to aortic dissection and ruptured atherosclerotic plaques [69,70], and the increase of endothelial protein C receptor (PROCR) in E-cig AE-treated cells, implying risks of vascular remodeling and atherosclerosis progression. *PROCR* expression is virtually absent in quiescent SMCs and significantly upregulated upon the homodimer platelet-derived growth factor-BB stimulation, with a probable role in restenosis and inward remodeling [71].

The close functional correlation, among KLF4, MMPs, and ILs, as evidenced by the DINs, underscores how the modulation of even one or few of them may have significant repercussions on the others. All these factors are downregulated in E-cig AE-treated HASMCs. Apparently, E-cig AE does not induce transdifferentiation of HASMCs into a non-contractile inflammatory phenotype, or at least, not through the same pathways modulated by TC AE.

Although the various AEs we tested induced distinct patterns of gene expression and protein abundance, interactome analysis revealed that the factors modulated by AEs are closely interconnected. Consequently, different active molecules or their different combinations, present in the three AEs, may trigger similar responses but through distinct pathways or biochemical processes (Table 2). Our data indicate that the water-soluble constituents of TC, E-cig, and THP actively impact HASMCs and induce a range of biochemical and behavioral responses critical to CVD progression. They also offer new insights into the molecular basis of various CV disorders, particularly regarding the onset and progression of atherosclerotic lesions.

5. Conclusions

Cigarette smoking is a major risk factor for CVDs, including atherosclerosis and stroke [72]. Our study examined the effects of TC, E-cig, and THP AEs on HASMCs (Fig. 4, graphical abstract).

TC AE induced a pro-inflammatory and pro-degradative environment by increasing IL1β and MMP3. E-cig AE suppressed inflammatory markers and *MMP* expression, potentially reducing plaque rupture risk, but increased proliferation and migration, raising concerns about vascular remodeling and fibrosis. THP AE showed intermediate effects.

Mitochondrial dysfunction and oxidative stress emerged as key drivers of AE-induced phenotypic changes, with alterations in critical metabolic enzymes (e.g., IDH3A, COX4I1). Differential regulation of cytokines, transcription factors, and ECM proteins were linked to

Table 2
Comparison of the effects of TC, E-cig, and THP AEs on cultured HASMCs.

Parameters	TC AE	E-cig AE	THP AE
Contractile Phenotype	Induces *ACTA2* and *MYOCD*.	Induces *ACTA2* and *MYOCD*; reduces *KLF4*.	Similar effects as TC and E-cig.
Synthetic Phenotype	Upregulates ECM components (COL1A1, FN1, DCN, LUM).	Upregulates ECM components, with an increased risk of fibrosis and vascular stiffness.	Upregulates ECM components with intermediate effects between TC and E-cig.
MMPs (ECM Degradation)	Upregulates MMPs, inducing a pro-degradative environment that destabilizes plaque structure.	Reduces MMP genes and proteins (particularly MMP3), potentially reducing the risk of plaque rupture.	Upregulates *MMP2* and *MMP3*; increases MMP3 protein, but reduces other MMPs, resulting in a less degradative environment compared to TC.
Oxidative Stress	Increases *HMOX1*, leading to ROS generation and potential ferroptosis.	Reduces IDH3A levels; risk of ECM accumulation and vascular stiffness.	Similar to E-cig for COX4I1 and IDH3A, with a risk of calcification and oxidative stress.
Inflammation	Increases *IL1β, IL6, IL8*, and IL1β protein expression, promoting pro-inflammatory responses associated with atherosclerosis.	Reduces inflammation and upregulates CHRNA7 (anti-inflammatory response). ROCK2 increased, indicating a pro-fibrotic effect.	Intermediate effects; ROCK2 is upregulated.
Proliferation (PCNA)	Significantly reduces PCNA expression and protein levels (reduced proliferation).	Significantly enhances PCNA expression, suggesting increased cellular proliferation.	Intermediate effects; moderate increase in PCNA expression and protein levels.
Migration (RAC1)	Reduces migration. RAC1 protein levels increase, but gene expression is reduced.	Significantly enhances migration (wound healing assay). Both RAC1 protein levels and gene expression are increased.	Migration is not significantly affected, but RAC1 expression and protein levels are moderately increased.
Vascular Calcification	Increases *ACTA2* and *MMP3*, associated with vascular calcification. *HMOX1* upregulation contributes to mitochondrial dysfunction and oxidative stress.	MMP3 downregulation may limit calcification, but there is a risk of ECM accumulation and vascular stiffness.	Similar to E-cig, with increased risk of calcification linked to ROS generation and altered metabolism.
Vascular Remodeling	Reduces EFEMP1 levels and increases PROCR expression, contributing to plaque instability and vascular dysfunction.	Increases proliferation and migration while reducing EFEMP1 levels; potential risk for vascular remodeling and fibrosis.	Increased PROCR levels; intermediate risk for vascular remodeling and fibrosis between TC and E-cig.

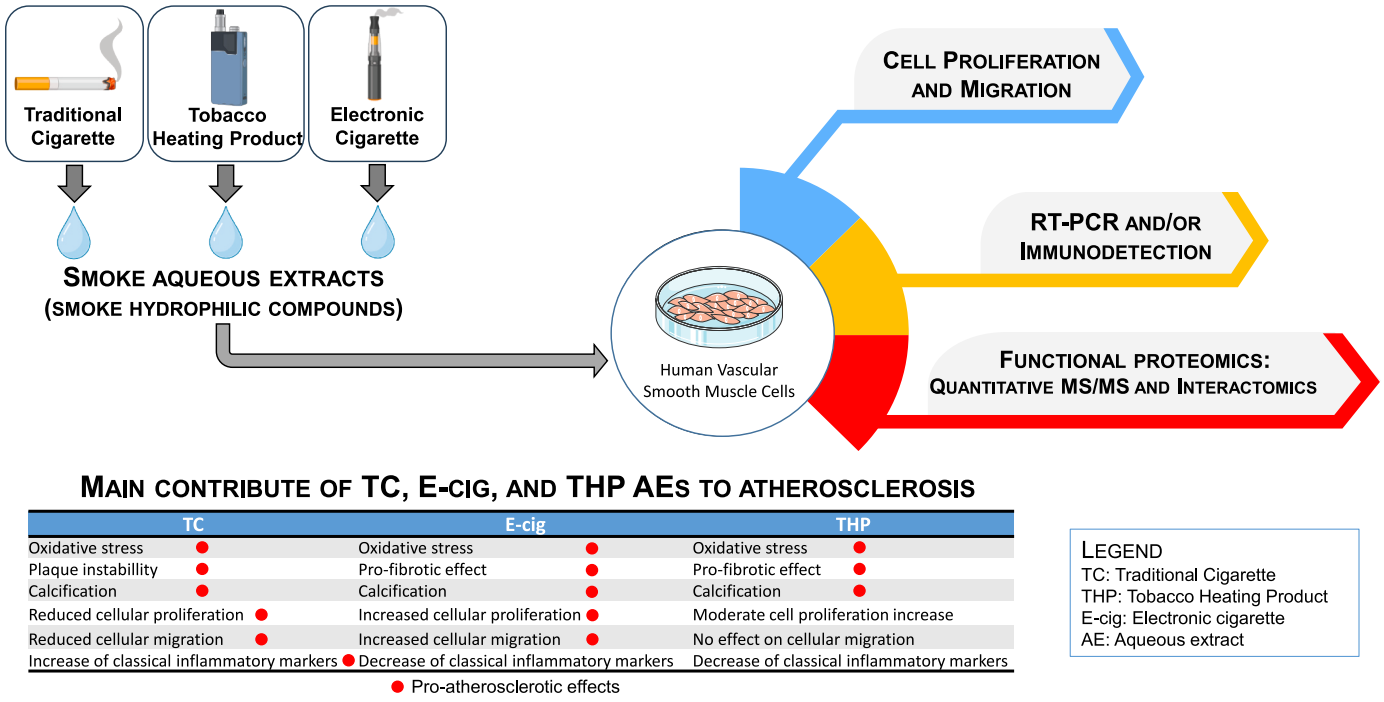

Fig. 4. TC AE induced a pro-inflammatory and pro-degradative environment. E-cig AE suppressed inflammatory markers, but increased proliferation and migration. THP AE showed intermediate effects.

distinct pathways promoting vascular remodeling and calcification.

While E-cigs and THPs may mitigate some harms of tobacco combustion, their potential to induce calcification, fibrosis, and neointimal hyperplasia necessitates further investigation to assess their actual long-term cardiovascular implications.

CRediT authorship contribution statement

L. Bianchi: Formal analysis, Validation, Writing – original draft, Writing – review & editing. **I. Damiani:** Investigation. **R. De Salvo:** Visualization, Formal analysis. **C. Rossi:** Visualization, Formal analysis. **A. Carleo:** Software, Formal analysis. **C. D'Alonzo:** Methodology, Formal analysis. **L. Bini:** Writing – review & editing. **A. Corsini:** Writing – review & editing. **S. Bellosta:** Conceptualization, Validation, Funding acquisition, Project administration, Writing – original draft, Writing – review & editing.

Financial support

Part of this work was supported by an educational grant from British American Tobacco (Southampton, UK).

Declaration of competing interest

The authors declare the following financial interests/personal relationships which may be considered as potential competing interests: Stefano Bellosta reports supplies was provided by British American Tobacco Research and Development. If there are other authors, they declare that they have no known competing financial interests or personal relationships that could have appeared to influence the work reported in this paper.

Acknowledgements

We thank British American Tobacco (Southampton, UK) for kindly providing us with the cigarette smoke aqueous extracts.

Appendix A. Supplementary data

Supplementary data to this article can be found online at https://doi.org/10.1016/j.atherosclerosis.2025.120412.

References

[1] Bennett MR, Sinha S, Owens GK. Vascular smooth muscle cells in atherosclerosis. Circ Res 2016;118:692–702. https://doi.org/10.1161/CIRCRESAHA.115.306361.
[2] Gomez D, Owens GK. Smooth muscle cell phenotypic switching in atherosclerosis. Cardiovasc Res 2012;95:156–64. https://doi.org/10.1093/cvr/cvs115.
[3] Owens GK. Regulation of differentiation of vascular smooth muscle cells. Physiol Rev 1995;75:487–517. https://doi.org/10.1152/physrev.1995.75.3.487.
[4] Allahverdian S, Chaabane C, Boukais K, Francis GA, Bochaton-Piallat ML. Smooth muscle cell fate and plasticity in atherosclerosis. Cardiovasc Res 2018;114:540–50. https://doi.org/10.1093/cvr/cvy022.
[5] Wirka RC, Wagh D, Paik DT, Pjanic M, Nguyen T, Miller CL, Kundu R, Nagao M, Coller J, Koyano TK, Fong R, Woo YJ, Liu B, Montgomery SB, Wu JC, Zhu K, Chang R, Alamprese M, Tallquist MD, Kim JB, Quertermous T. Atheroprotective roles of smooth muscle cell phenotypic modulation and the TCF21 disease gene as revealed by single-cell analysis. Nat Med 2019;25:1280–9. https://doi.org/10.1038/s41591-019-0512-5.
[6] Allahverdian S, Pannu PS, Francis GA. Contribution of monocyte-derived macrophages and smooth muscle cells to arterial foam cell formation. Cardiovasc Res 2012;95:165–72. https://doi.org/10.1093/cvr/cvs094.
[7] Ross R. Atherosclerosis — an inflammatory disease. N Engl J Med 1999;340:115–26. https://doi.org/10.1056/NEJM199901143400207.
[8] Rong JX, Shapiro M, Trogan E, Fisher EA. Transdifferentiation of mouse aortic smooth muscle cells to a macrophage-like state after cholesterol loading. Proc Natl Acad Sci 2003;100:13531–6. https://doi.org/10.1073/pnas.1735526100.
[9] Allahverdian S, Pannu PS, Francis GA. Contribution of monocyte-derived macrophages and smooth muscle cells to arterial foam cell formation. Cardiovasc Res 2012;95:165–72. https://doi.org/10.1093/CVR/CVS094.
[10] Kim JB, Zhao Q, Nguyen T, Pjanic M, Cheng P, Wirka R, Travisano S, Nagao M, Kundu R, Quertermous T. Environment-sensing aryl hydrocarbon receptor inhibits the chondrogenic fate of modulated smooth muscle cells in atherosclerotic lesions. Circulation 2020;142:575–90. https://doi.org/10.1161/CIRCULATIONAHA.120.045981.
[11] Bianchi L, Damiani I, Castiglioni S, Carleo A, De Salvo R, Rossi C, Corsini A, Bellosta S. Smooth muscle cell phenotypic switch induced by traditional cigarette

smoke condensate: a holistic overview. Int J Mol Sci 2023;24:6431. https://doi.org/10.3390/ijms24076431.
[12] Virdis A, Giannarelli C, Neves MF, Taddei S, Ghiadoni L. Cigarette smoking and hypertension. Curr Pharm Des 2010;16:2518–25. https://doi.org/10.2174/138161210792062920.
[13] Tilp C, Bucher H, Haas H, Duechs MJ, Wex E, Erb KJ. Effects of conventional tobacco smoke and nicotine-free cigarette smoke on airway inflammation, airway remodelling and lung function in a triple allergen model of severe asthma. Clin Exp Allergy 2016;46:957–72. https://doi.org/10.1111/cea.12665.
[14] Cullen KA, Gentzke AS, Sawdey MD, Chang JT, Anic GM, Wang TW, Creamer MLR, Jamal A, Ambrose BK, King BA. e-Cigarette use among youth in the United States, 2019. JAMA, J Am Med Assoc 2019;322:2095–103. https://doi.org/10.1001/jama.2019.18387.
[15] Ebersole J, Samburova V, Son Y, Cappelli D, Demopoulos C, Capurro A, Pinto A, Chrzan B, Kingsley K, Howard K, Clark N, Khlystov A. Harmful chemicals emitted from electronic cigarettes and potential deleterious effects in the oral cavity. Tob Induc Dis 2020;18:1–16. https://doi.org/10.18332/TID/116988.
[16] Eaton DL, Kwan LY, Stratton K. In: Public health consequences of E-cigarettes; 2018. https://doi.org/10.17226/24952. Washington (DC).
[17] Lee J, Yao Z, Boakye E, Blaha MJ. The impact of chronic electronic cigarette use on endothelial dysfunction measured by flow-mediated vasodilation: a systematic review and meta-analysis. Tob Induc Dis 2024;22. https://doi.org/10.18332/TID/186932.
[18] El-Mahdy MA, Ewees MG, Eid MS, Mahgoup EM, Khaleel SA, Zweier JL. Electronic cigarette exposure causes vascular endothelial dysfunction due to NADPH oxidase activation and eNOS uncoupling. Am J Physiol Heart Circ Physiol 2022;322:H549–67. https://doi.org/10.1152/AJPHEART.00460.2021.
[19] Gernun S, Franzen KF, Mallock N, Benthien J, Luch A, Mortensen K, Drömann D, Pogarell O, Rüther T, Rabenstein A. Cardiovascular functions and arterial stiffness after JUUL use. Tob Induc Dis 2022;20. https://doi.org/10.18332/TID/144317.
[20] Carll AP, Arab C, Salatini R, Miles MD, Nystoriak MA, Fulghum KL, Riggs DW, Shirk GA, Theis WS, Talebi N, Bhatnagar A, Conklin DJ. E-cigarettes and their lone constituents induce cardiac arrhythmia and conduction defects in mice. Nat Commun 2022;13. https://doi.org/10.1038/S41467-022-33203-1.
[21] Kim SY, Jeong SH, Joo HJ, Park M, Park EC, Kim JH, Lee J, Shin J. High prevalence of hypertension among smokers of conventional and e-cigarette: using the nationally representative community dwelling survey. Front Public Health 2022;10. https://doi.org/10.3389/FPUBH.2022.919585.
[22] Lempert LK, Glantz SA. Heated tobacco product regulation under US law and the FCTC. Tob Control 2018;27:s118–25. https://doi.org/10.1136/tobaccocontrol-2018-054560.
[23] Ioakeimidis N, Emmanouil E, Terentes-Printzios D, Dima I, Aznaouridis K, Tousoulis D, Vlachopoulos C. Acute effect of heat-not-burn versus standard cigarette smoking on arterial stiffness and wave reflections in young smokers. Eur J Prev Cardiol 2021;28:E9–11. https://doi.org/10.1177/2047487320918365.
[24] Biondi-Zoccai G, Sciarretta S, Bullen C, Nocella C, Violi F, Loffredo L, Pignatelli P, Perri L, Peruzzi M, Marullo AGM, De Falco E, Chimenti I, Cammisotto V, Valenti V, Coluzzi F, Cavarretta E, Carrizzo A, Prati F, Carnevale R, Frati G. Acute effects of heat-not-burn, electronic vaping, and traditional tobacco combustion cigarettes: the sapienza university of rome-vascular assessment of proatherosclerotic effects of smoking (SUR-VAPES) 2 randomized trial. J Am Heart Assoc 2019;8. https://doi.org/10.1161/JAHA.118.010455.
[25] Bozhilova S, Baxter A, Bishop E, Breheny D, Thorne D, Hodges P, Gaça M. Optimization of aqueous aerosol extract (AqE) generation from e-cigarettes and tobacco heating products for in vitro cytotoxicity testing. Toxicol Lett 2020;335:51–63. https://doi.org/10.1016/j.toxlet.2020.10.005.
[26] Bianchi L, Bruzzese F, Leone A, Gagliardi A, Puglia M, Di Gennaro E, Rocco M, Gimigliano A, Pucci B, Armini A, Bini L, Budillon A. Proteomic analysis identifies differentially expressed proteins after HDAC vorinostat and EGFR inhibitor gefitinib treatments in Hep-2 cancer cells. Proteomics 2011;11:3725–42. https://doi.org/10.1002/PMIC.201100092.
[27] Accattatis FM, Caruso A, Carleo A, Del Console P, Gelsomino L, Bonofiglio D, Giordano C, Barone I, Andò S, Bianchi L, Catalano S. CEBP-β and PLK1 as potential mediators of the breast cancer/obesity crosstalk: in vitro and in silico analyses. Nutrients 2023;15. https://doi.org/10.3390/NU15132839.
[28] Vantaggiato L, Shaba E, Carleo A, Bezzini D, Pannuzzo G, Luddi A, Piomboni P, Bini L, Bianchi L. Neurodegenerative disorder risk in krabbe disease carriers. Int J Mol Sci 2022;23. https://doi.org/10.3390/IJMS232113537.
[29] Bini L, Schvartz D, Carnemolla C, Besio R, Garibaldi N, Sanchez JC, Forlino A, Bianchi L. Intracellular and extracellular markers of lethality in osteogenesis imperfecta: a quantitative proteomic approach. Int J Mol Sci 2021;22:1–23. https://doi.org/10.3390/IJMS22010429.
[30] Strzalka W, Ziemienowicz A. Proliferating cell nuclear antigen (PCNA): a key factor in DNA replication and cell cycle regulation. Ann Bot 2011;107:1127–40. https://doi.org/10.1093/aob/mcq243.
[31] Gerthoffer WT. Mechanisms of vascular smooth muscle cell migration. Circ Res 2007;100:607–21. https://doi.org/10.1161/01.RES.0000258492.96097.47.
[32] Spiering D, Hodgson L. Dynamics of the rho-family small GTPases in actin regulation and motility. Cell Adhes Migrat 2011;5:170–80. https://doi.org/10.4161/cam.5.2.14403.
[33] Ren C, Tong Y, Li J, Lu Z, Yao Y. The protective effect of alpha 7 nicotinic acetylcholine receptor activation on critical illness and its mechanism. Int J Biol Sci 2017;13:46–56. https://doi.org/10.7150/ijbs.16404.
[34] Yoshiyama S, Chen Z, Okagaki T, Kohama K, Nasu-Kawaharada R, Izumi T, Ohshima N, Nagai T, Nakamura A. Nicotine exposure alters human vascular smooth muscle cell phenotype from a contractile to a synthetic type. Atherosclerosis 2014;237:464–70. https://doi.org/10.1016/j.atherosclerosis.2014.10.019.
[35] Schraufstatter IU, DiScipio RG, Khaldoyanidi SK. Alpha 7 subunit of nAChR regulates migration of human mesenchymal stem cells. J Stem Cell 2009;4:203–15. https://doi.org/jsc.2010.4.4.203.
[36] Adamson J, Azzopardi D, Errington G, Dickens C, McAughey J, Gaça MD. Assessment of an in vitro whole cigarette smoke exposure system: the borgwaldt RM20S 8-syringe smoking machine. Chem Cent J 2011;5. https://doi.org/10.1186/1752-153X-5-50.
[37] Fearon IM, Gaça MD, Nordskog BK. In vitro models for assessing the potential cardiovascular disease risk associated with cigarette smoking. Toxicol Vitro 2013;27:513–22. https://doi.org/10.1016/J.TIV.2012.08.018.
[38] Yoshida T, Sinha S, Dandré F, Wamhoff BR, Hoofnagle MH, Kremer BE, Wang DZ, Olson EN, Owens GK. Myocardin is a key regulator of CArG-dependent transcription of multiple smooth muscle marker genes. Circ Res 2003;92:856–64. https://doi.org/10.1161/01.RES.0000068405.49081.09.
[39] Liu Y, Sinha S, McDonald OG, Shang Y, Hoofnagle MH, Owens GK. Kruppel-like factor 4 abrogates myocardin-induced activation of smooth muscle gene expression. J Biol Chem 2005;280:9719–27. https://doi.org/10.1074/JBC.M412862200.
[40] Chen R, McVey DG, Shen D, Huang X, Ye S. Phenotypic switching of vascular smooth muscle cells in atherosclerosis. J Am Heart Assoc 2023;12. https://doi.org/10.1161/JAHA.123.031121.
[41] Ignatieva E, Kostina D, Irtyuga O, Uspensky V, Golovkin A, Gavriliuk N, Moiseeva O, Kostareva A, Malashicheva A. Mechanisms of smooth muscle cell differentiation are distinctly altered in thoracic aortic aneurysms associated with bicuspid or tricuspid aortic valves. Front Physiol 2017;8. https://doi.org/10.3389/FPHYS.2017.00536.
[42] Shanahan CM, Weissberg PL. Smooth muscle cell heterogeneity: patterns of gene expression in vascular smooth muscle cells in vitro and in vivo. Arterioscler Thromb Vasc Biol 1998;18:333–8. https://doi.org/10.1161/01.ATV.18.3.333.
[43] Matheson C, Simovic T, Heefner A, Colon M, Tunon E, Cobb K, Thode C, Breland A, Cobb CO, Nana-Sinkam P, Garten R, Rodriguez-Miguelez P. Evidence of premature vascular dysfunction in young adults who regularly use e-cigarettes and the impact of usage length. Angiogenesis 2024;27:229–43. https://doi.org/10.1007/S10456-023-09903-7.
[44] Xie Y, Lin T, Jin Y, Berezowitz AG, Wang XL, Lu J, Cai Y, Guzman RJ. Smooth muscle cell-specific matrix metalloproteinase 3 deletion reduces osteogenic transformation and medial artery calcification. Cardiovasc Res 2024;120:658–70. https://doi.org/10.1093/CVR/CVAE035.
[45] Chi C, Li DJ, Jiang YJ, Tong J, Fu H, Wu YH, Shen FM. Vascular smooth muscle cell senescence and age-related diseases: state of the art. Biochim Biophys Acta Mol Basis Dis 2019;1865:1810–21. https://doi.org/10.1016/J.BBADIS.2018.08.015.
[46] Khanal S, Bhavnani N, Mathias A, Lallo J, Gupta S, Ohanyan V, Ferrell JM, Raman P. Deletion of smooth muscle O-GlcNAc transferase prevents development of atherosclerosis in Western diet-fed hyperglycemic ApoE-/- mice in vivo. Int J Mol Sci 2023;24. https://doi.org/10.3390/IJMS24097899.
[47] Chen Y, Zhao X, Wu H. Metabolic stress and cardiovascular disease in diabetes mellitus: the role of protein O-GlcNAc modification. Arterioscler Thromb Vasc Biol 2019;39:1911–24. https://doi.org/10.1161/ATVBAHA.119.312192.
[48] Liu S, He L, Yao K. The antioxidative function of alpha-ketoglutarate and its applications. BioMed Res Int 2018;2018. https://doi.org/10.1155/2018/3408467.
[49] Blacker TS, Duchen MR. Investigating mitochondrial redox state using NADH and NADPH autofluorescence. Free Radic Biol Med 2016;100:53–65. https://doi.org/10.1016/J.FREERADBIOMED.2016.08.010.
[50] Meng Z, Liang H, Zhao J, Gao J, Liu C, Ma X, Liu J, Liang B, Jiao X, Cao J, Wang Y. HMOX1 upregulation promotes ferroptosis in diabetic atherosclerosis. Life Sci 2021;284. https://doi.org/10.1016/J.LFS.2021.119935.
[51] Zdzisińska B, Żurek A, Kandefer-Szerszeń M. Alpha-ketoglutarate as a molecule with pleiotropic activity: well-known and novel possibilities of therapeutic use. Arch Immunol Ther Exp 2017;65:21–36. https://doi.org/10.1007/S00005-016-0406-X.
[52] Balogh E, Tóth A, Méhes G, Trencsényi G, Paragh G, Jeney V. Hypoxia triggers osteochondrogenic differentiation of vascular smooth muscle cells in an HIF-1 (Hypoxia-Inducible factor 1)-Dependent and reactive oxygen species-dependent manner. Arterioscler Thromb Vasc Biol 2019;39:1088–99. https://doi.org/10.1161/ATVBAHA.119.312509.
[53] Pajuelo Reguera D, Čunátová K, Vrbacký M, Pecinová A, Houštěk J, Mráček T, Pecina P. Cytochrome c oxidase subunit 4 isoform exchange results in modulation of oxygen affinity. Cells 2020;9. https://doi.org/10.3390/CELLS9020443.
[54] Barua RS, Sharma M, Dileepan KN. Cigarette smoke amplifies inflammatory response and atherosclerosis progression through activation of the H1R-TLR2/4-COX2 axis. Front Immunol 2015;6:164567. https://doi.org/10.3389/FIMMU.2015.00572/BIBTEX.
[55] Jiang H, Guo Z, Zeng K, Tang H, Tan H, Min R, Huang C. IL-1β knockdown inhibits cigarette smoke extract-induced inflammation and apoptosis in vascular smooth muscle cells. PLoS One 2023;18:e0277719. https://doi.org/10.1371/JOURNAL.PONE.0277719.
[56] Takeda Y, Matoba K, Kawanami D, Nagai Y, Akamine T, Ishizawa S, Kanazawa Y, Yokota T, Utsunomiya K. ROCK2 regulates monocyte migration and cell to cell adhesion in vascular endothelial cells. Int J Mol Sci 2019;20. https://doi.org/10.3390/IJMS20061331.
[57] Li Y, Tai HC, Sladojevic N, Kim HH, Liao JK. Vascular stiffening mediated by rho-associated coiled-coil containing kinase isoforms. J Am Heart Assoc 2021;10. https://doi.org/10.1161/JAHA.121.022568.

[58] Shimizu T, Fukumoto Y, Tanaka SI, Satoh K, Ikeda S, Shimokawa H. Crucial role of ROCK2 in vascular smooth muscle cells for hypoxia-induced pulmonary hypertension in mice. Arterioscler Thromb Vasc Biol 2013;33:2780–91. https://doi.org/10.1161/ATVBAHA.113.301357.
[59] Yu B, Sladojevic N, Blair JE, Liao JK. Targeting Rho-associated coiled-coil forming protein kinase (ROCK) in cardiovascular fibrosis and stiffening. Expert Opin Ther Targets 2020;24:47–62. https://doi.org/10.1080/14728222.2020.1712593.
[60] Eun SY, Ko YS, Park SW, Chang KC, Kim HJ. IL-1β enhances vascular smooth muscle cell proliferation and migration via P2Y2 receptor-mediated RAGE expression and HMGB1 release. Vasc Pharmacol 2015;72:108–17. https://doi.org/10.1016/j.vph.2015.04.013.
[61] Yoshiyama S, Horinouchi T, Miwa S, Wang HH, Kohama K, Nakamura A. Effect of cigarette smoke components on vascular smooth muscle cell migration toward platelet-derived growth factor BB. J Pharmacol Sci 2011;115:532–5. https://doi.org/10.1254/jphs.10283SC.
[62] de Lima JM, Macedo CCS, Barbosa GV, Castellano LRC, Hier MP, Alaoui-Jamali MA, da Silva SD. E-liquid alters oral epithelial cell function to promote epithelial to mesenchymal transition and invasiveness in preclinical oral squamous cell carcinoma. Sci Rep 2023;13. https://doi.org/10.1038/S41598-023-30016-0.
[63] Almeda J, Chinnaiyan V, Andl C. Abstract 1437: E-Cigarette vape promotes cell cycle progression and inflammation in 3D pre-clinical oral spheroid models. Cancer Res 2023;83. https://doi.org/10.1158/1538-7445.AM2023-1437.
[64] Liu Q, Zhao M, Chen W, Xu K, Huang F, Qu J, Xu Z, Wang X, Wang Y, Zhu Y, Wang W. Mainstream cigarette smoke induces autophagy and promotes apoptosis in oral mucosal epithelial cells. Arch Oral Biol 2020;111. https://doi.org/10.1016/J.ARCHORALBIO.2019.104646.
[65] Ueda K, Sakai C, Ishida T, Morita K, Kobayashi Y, Horikoshi Y, Baba A, Okazaki Y, Yoshizumi M, Tashiro S, Ishida M. Cigarette smoke induces mitochondrial DNA damage and activates cGAS-STING pathway: application to a biomarker for atherosclerosis. Clin Sci (Lond) 2023;137:163–80. https://doi.org/10.1042/CS20220525.
[66] Taylor M, Jaunky T, Hewitt K, Breheny D, Lowe F, Fearon IM, Gaca M. A comparative assessment of e-cigarette aerosols and cigarette smoke on in vitro endothelial cell migration. Toxicol Lett 2017;277:123–8. https://doi.org/10.1016/J.TOXLET.2017.06.001.
[67] Spiering D, Hodgson L. Dynamics of the rho-family small GTPases in actin regulation and motility. Cell Adhes Migrat 2011;5:170–80. https://doi.org/10.4161/CAM.5.2.14403.
[68] Zhang L, Gallup M, Zlock L, Finkbeiner WE, McNamara NA. Rac1 and Cdc42 differentially modulate cigarette smoke-induced airway cell migration through p120-catenin-dependent and -independent pathways. Am J Pathol 2013;182:1986–95. https://doi.org/10.1016/J.AJPATH.2013.02.008.
[69] Zhi K, Yin R, Guo H, Qu L. PUM2 regulates the formation of thoracic aortic dissection through EFEMP1. Exp Cell Res 2023;427. https://doi.org/10.1016/J.YEXCR.2023.113602.
[70] Xu BF, Liu R, Huang CX, He BS, Li GY, Sun HS, Feng ZP, Bao MH. Identification of key genes in ruptured atherosclerotic plaques by weighted gene correlation network analysis. Sci Rep 2020;10. https://doi.org/10.1038/S41598-020-67114-2.
[71] Lee MY, Garvey SM, Ripley ML, Wamhoff BR. Genome-wide microarray analyses identify the protein C receptor as a novel calcineurin/nuclear factor of activated T cells-dependent gene in vascular smooth muscle cell phenotypic modulation. Arterioscler Thromb Vasc Biol 2011;31:2665–75. https://doi.org/10.1161/ATVBAHA.111.235960.
[72] Rose JJ, Krishnan-Sarin S, Exil VJ, Hamburg NM, Fetterman JL, Ichinose F, Perez-Pinzon MA, Rezk-Hanna M, Williamson E. Cardiopulmonary impact of electronic cigarettes and vaping products: a scientific statement from the American heart association. Circulation 2023;148:703–28. https://doi.org/10.1161/CIR.0000000000001160.